

AD-A194 057

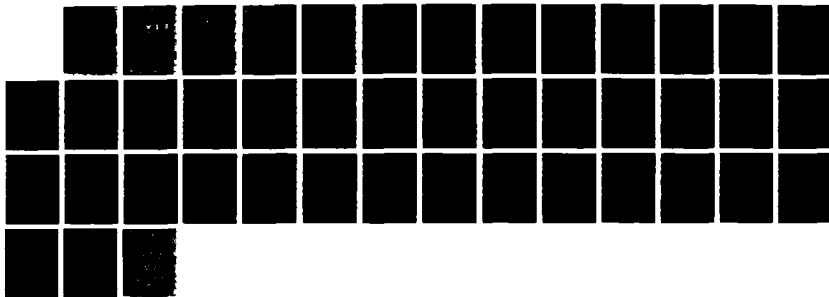
A NUMERICAL STUDY OF THE TEST TIME IN A HYPERSONIC
SHOCK TUNNEL(U) AIR COMMAND AND STAFF COLL MAXWELL AFB
AL R E DILLON APR 88 ACSC-88-0740

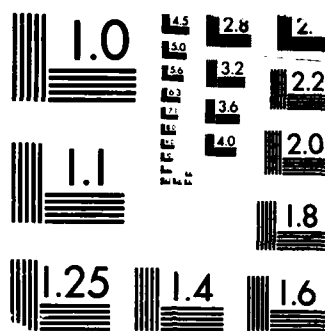
1/1

UNCLASSIFIED

F/G 20/4

NL





MICROCOPY RESOLUTION TEST CHART
NBS 1963-A

AD-A194 057

DTIC FILE COPY

2



DTIC
ELECTE
JUN 10 1988
S H D

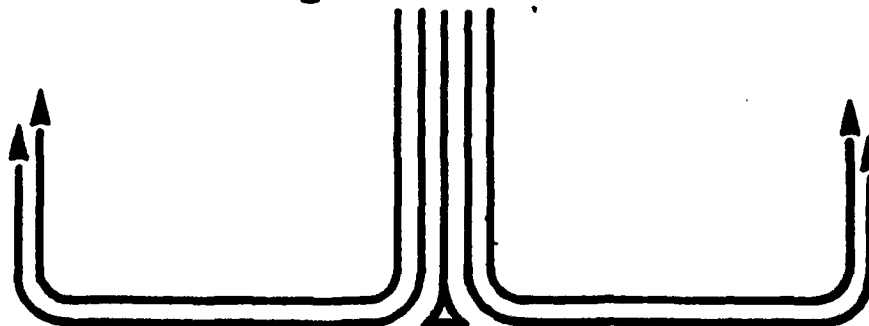
AIR COMMAND AND STAFF COLLEGE

STUDENT REPORT

A NUMERICAL STUDY OF THE
TEST TIME IN A HYPERSONIC SHOCK TUNNEL

MAJOR ROBERT E. DILLON, JR. 88-0740

"insights into tomorrow"



DISTRIBUTION STATEMENT A

Approved for public release;
Distribution Unlimited

88 6 6 053



REPORT NUMBER 88-0740

TITLE A NUMERICAL STUDY OF THE TEST TIME IN A HYPERSONIC SHOCK TUNNEL

AUTHOR(S) MAJOR ROBERT E. DILLON, JR., USA

FACULTY ADVISOR LT COL LARRY G. ROSELAND, ACSC/EDW

SPONSOR DR. HENRY T. NAGAMATSU, PROFESSOR OF AERONAUTICAL ENGINEERING
RENSSELAER POLYTECHNIC INSTITUTE, TROY, NEW YORK

Submitted to the faculty in partial fulfillment of
requirements for graduation.

AIR COMMAND AND STAFF COLLEGE
AIR UNIVERSITY
MAXWELL AFB, AL 36112-5542

UNCLASSIFIED

SECURITY CLASSIFICATION OF THIS PAGE

REPORT DOCUMENTATION PAGE				Form Approved OMB No. 0704-0188	
1a. REPORT SECURITY CLASSIFICATION UNCLASSIFIED			1b. RESTRICTIVE MARKINGS		
2a. SECURITY CLASSIFICATION AUTHORITY			3. DISTRIBUTION / AVAILABILITY OF REPORT STATEMENT "A" Approved for public release; Distribution is unlimited.		
2b. DECLASSIFICATION / DOWNGRADING SCHEDULE					
4. PERFORMING ORGANIZATION REPORT NUMBER(S) 88-0740			5. MONITORING ORGANIZATION REPORT NUMBER(S)		
6a. NAME OF PERFORMING ORGANIZATION ACSC/EDC		6b. OFFICE SYMBOL (If applicable)	7a. NAME OF MONITORING ORGANIZATION		
6c. ADDRESS (City, State, and ZIP Code) Maxwell AFB AL 36112-5542			7b. ADDRESS (City, State, and ZIP Code)		
8a. NAME OF FUNDING / SPONSORING ORGANIZATION		8b. OFFICE SYMBOL (If applicable)	9. PROCUREMENT INSTRUMENT IDENTIFICATION NUMBER		
8c. ADDRESS (City, State, and ZIP Code)			10. SOURCE OF FUNDING NUMBERS		
			PROGRAM ELEMENT NO.	PROJECT NO.	TASK NO.
11. TITLE (Include Security Classification) A NUMERICAL STUDY OF THE TEST TIME IN A HYPERSONIC SHOCK TUNNEL					
12. PERSONAL AUTHOR(S) Dillon, Robert E., Jr., Major, USA					
13a. TYPE OF REPORT		13b. TIME COVERED FROM _____ TO _____		14. DATE OF REPORT (Year, Month, Day) 1988 April	
15. PAGE COUNT 42					
16. SUPPLEMENTARY NOTATION					
17. COSATI CODES			18. SUBJECT TERMS (Continue on reverse if necessary and identify by block number)		
FIELD	GROUP	SUB-GROUP			
19. ABSTRACT (Continue on reverse if necessary and identify by block number) A numerical study was made of the test time in a hypersonic shock tunnel for Mach 10 flow. Harten's total variation diminishing (TVD) scheme was used to simulate the entire shock tunnel operation from diaphragm rupture to disruption of the flow in the nozzle. The code was able to model the main features of unsteady flow in a shock tube to include the shock wave and contact surface intersections. Results were obtained that predict the steady flow duration time for stagnation temperatures of 1200°F, 2700°F, and 6900°F. Both air and helium were used as driver gases with air as the test gas.					
20. DISTRIBUTION / AVAILABILITY OF ABSTRACT <input type="checkbox"/> UNCLASSIFIED/UNLIMITED <input checked="" type="checkbox"/> SAME AS RPT. <input type="checkbox"/> DTIC USERS			21. ABSTRACT SECURITY CLASSIFICATION UNCLASSIFIED		
22a. NAME OF RESPONSIBLE INDIVIDUAL ACSC/EDC Maxwell AFB AL 36112-5542			22b. TELEPHONE (Include Area Code) (205) 293-2867		22c. OFFICE SYMBOL

PREFACE

This paper was written expressly for Professor Henry T. Nagamatsu, Professor of Aeronautical Engineering, Rensselaer Polytechnic Institute, Troy, New York. The length limitation of the paper prohibited a detailed discussion on the elementary principles of shock tube operation and other gas dynamic phenomena. For this reason, readers unfamiliar with these concepts should first begin with a thorough review of the principles of unsteady, one dimensional gas dynamics. An excellent text for this is Gas Dynamics, 2nd ed. by James E. A. John, Allyn and Bacon, Inc. Newton, MA, 1984. Also, readers unfamiliar with the elements of computational fluid dynamics should begin with a review of these elements. An excellent text for this is Reference 1.

I am extremely grateful to Dr. Gary Carofano of the US Army's Benet Weapons Laboratory for the work he did in applying Harten's scheme to an easily workable computer code. In addition, his many informative and stimulating discussions led to an easier understanding of the complications of CFD limitations, the thermodynamics of the problem, and an overall better understanding of these phenomena. His patience and depth of understanding are greatly appreciated.



Accession For	
NTIS GRA&I	<input checked="" type="checkbox"/>
DTIC TAB	<input type="checkbox"/>
Unannounced	<input type="checkbox"/>
Justification	
By	
Distribution/	
Availability Codes	
Dist	Avail and/or Special
A-1	

ABOUT THE AUTHOR

Major Robert E. Dillon, Jr. was commissioned from the United States Military Academy as a Second Lieutenant of armor in 1974. He served as a Platoon Leader, Company Executive Officer and Company Commander with a tank battalion in the Federal Republic of Germany from 1975 to 1979. He returned to the United States and obtained his PhD in Aeronautical Engineering from Rensselaer Polytechnic Institute. He served as Program Manager in the Armament Research and Development Command and then as an Associate Professor in the Department of Mechanics, US Military Academy. He is a graduate of the Army's Airborne School, Ranger School, Armor Officer Basic Course, Infantry Officer Advanced Course and the Command and General Staff College. He is licensed as a Professional Engineer in the Commonwealth of Virginia. A list of his publications follows.

- R. E. Dillon, "Heat Transfer Rate for Laminar, Transition, and Turbulent Boundary Layers and Transition Phenomena on Shock Tube Wall." ME Thesis, Rensselaer Polytechnic Institute, Troy, New York, 1981.
- R. E. Dillon and H. T. Nagamatsu, "Heat Transfer Rate for Laminar, Transition and Turbulent Boundary Layers and Transition Phenomena on Shock Tube Wall." Paper 82-0032 presented at the AIAA 20th Aerospace Science Meeting, Orlando, FL, January 11-14, 1982.
- R. E. Dillon, "A Method of Analyzing Perforated Muzzle Brake Performance." PhD dissertation, Rensselaer Polytechnic Institute, Troy, NY, 1983.
- R. E. Dillon and H. T. Nagamatsu, "A Method of Analyzing Perforated Muzzle Brake Performance." US Army Armament Research and Development Center Report ARLCB-TR-84003, Benet Weapons Laboratory, Watervliet, NY, 1984.
- R. E. Dillon and H. T. Nagamatsu, "An Experimental Study of Perforated Muzzle Brakes." US Army Armament Research and Development Center Report ARLCB-TR-84004, Benet Weapons Laboratory, Watervliet, NY, 1984.

- R. E. Dillon, "A Parametric Study of Perforated Muzzle Brakes." US Army Armament Research and Development Center Report ARLCB-TR-84015, Benet Weapons Laboratory, Watervliet, NY, 1984.
- R. E. Dillon, "Wall Thickness and Vent Area Effects on Perforated Muzzle Brake Performance." US Army Armament Research and Development Center Report ARLCB-TR-84020, Benet Weapons Laboratory, Watervliet, NY, 1984.
- R. E. Dillon and H. T. Nagamatsu, "An Experimental Study of Perforated Muzzle Brakes." paper 84-1642 presented at the AIAA 17th Fluid Dynamics, Plasma Dynamics and Lasers Conference, Snowmass, CO, June 25-27, 1984.
- R. E. Dillon and H. T. Nagamatsu, "Heat Transfer and Transition Mechanism on Shock Tube Wall." AIAA Journal, Vol. 22, No. 11, November 1984, 1524-1528.
- R. E. Dillon and M. A. Paolino, "The Thermal Response of Perforated Muzzle Brakes." US Army Armament Research and Engineering Center Report ARCCB-CR-87004, Benet Weapons Laboratory, Watervliet, NY, 1987.

TABLE OF CONTENTS

Preface.....	111
About the Author.....	iv
List of Illustrations.....	vii
Abstract.....	ix
CHAPTER ONE--INTRODUCTION	
Objective of the Study.....	1
Historical Background.....	1
Significance of the Problem.....	2
Ground Test Facilities.....	3
CHAPTER TWO--NUMERICAL METHODS FOR HYPERSONIC FLOW	
Assumptions and Limitations.....	9
Description of Numerical Method Used.....	9
CHAPTER THREE--DISCUSSION AND ANALYSIS OF NUMERICAL DATA	
Mach 2.3 Incident Shock	
Air Driver.....	13
Helium Driver.....	18
Mach 3.41 Incident Shock.....	19
Mach 5.4 Incident Shock.....	20
CHAPTER FOUR	
Conclusions.....	27
Recommendations.....	28
BIBLIOGRAPHY.....	29

LIST OF ILLUSTRATIONS

TABLES

TABLE 1--Comparison of Test Facilities.....	4
TABLE 2--Shock Tunnel Transducer Data.....	12
TABLE 3--Stagnation Temperature and Shock Mach Number.....	13
TABLE 4--Comparison of Test Times.....	27

FIGURES

FIGURE 1--Stagnation Temperature and Flow Duration Time for Test Facilities.....	5
FIGURE 2--Typical Wave Diagram for a Hypersonic Shock Tunnel.....	6
FIGURE 3--RPI Shock Tunnel Layout.....	11
FIGURE 4--Nozzle Section Layout and Transducer Locations.....	11
FIGURE 5--Static Pressure History Mach 10 (upper) and Mach 7.4 (lower). Mach 2.3 Incident Shock, Air Driver.....	14
FIGURE 6--Density History Mach 10 (upper) and Mach 7.4 (lower). Mach 2.3 Incident Shock, Air Driver.....	15
FIGURE 7--Probe Total Pressure History Mach 10 (upper) and Mach 7.4 (lower). Mach 2.3 Incident Shock, Air Driver.....	16
FIGURE 8--Mach Number and Pressure Distribution, 14.3 ms. Mach 2.3 Shock, Air Driver.....	17
FIGURE 9--Mach Number and Pressure Distribution, 21.5 ms. Mach 2.3 Shock, Air Driver.....	18
FIGURE 10--Mach Number and Pressure Distribution, 26 ms. Mach 2.3 Shock, Air Driver.....	19
FIGURE 11--Mach Number and Pressure Distribution, 28 ms. Mach 2.3 Shock, Air Driver.....	20
FIGURE 12--Mach Number and Pressure Distribution, 28 ms. Mach 2.3 Shock, Helium Driver...	21
FIGURE 13--Probe Total Pressure History Mach 10 (upper) and Mach 7.4 (lower). Mach 2.3 Incident Shock, Helium Driver.....	22
FIGURE 14--Wave Diagram for Shock Interactions.....	23

FIGURE 15--Mach Number and Pressure Distribution, 22 ms. Mach 3.41 Shock, Helium Driver..	24
FIGURE 16--Probe Total Pressure History Mach 10. Mach 3.41 Incident Shock.....	25
FIGURE 17--Static Pressure History Mach 10 (upper) and Mach 7.4 (lower). Mach 5.4 Incident Shock.....	26

ABSTRACT

A numerical study was made of the test time in a hypersonic shock tunnel for Mach 10 flow. Harten's total variation diminishing (TVD) scheme was used to simulate the entire shock tunnel operation from diaphragm rupture to disruption of the flow in the nozzle. The code was able to model the main features of unsteady flow in a shock tube to include the shock wave and contact surface intersections. Results were obtained that predict the steady flow duration time for stagnation temperatures of 1200°R, 2700°R, and 6000°R. Both air and helium were used as driver gases with air as the test gas.

Chapter One

INTRODUCTION

OBJECTIVE OF THE STUDY

This work was undertaken to accomplish two goals: to conduct a numerical analysis of the test time available in the Rensselaer Polytechnic Institute (RPI) hypersonic shock tunnel and determine the conditions yielding the maximum possible flow duration time.

HISTORICAL BACKGROUND

In the late 1950s and early 1960s much aeronautical research was being devoted to the high Mach number regime known as hypersonic (27:1). The research centered primarily on experimental (3,17-25,32,34-39,41,42) and analytical (16,26,29,30) work in support of such programs as Mercury, Gemini, Apollo, and X-15 for the National Aeronautics and Space Administration (NASA) and research on ballistic missile reentry vehicles for the Air Force and Navy (44:2). In the early 1970s, the X-15 and Apollo projects were completed, America's Supersonic Transport (SST) was killed by Congress, and the bulk of the design work for the space shuttle was completed. Few research dollars were available for hypersonic aerodynamics causing the effort in this area to stop (44:3). Virtually all of the hypersonic experimental research facilities in the United States fell into a state of disuse or were dismantled and sold for scrap (27:1). Until 1984 hypersonic research in the United States was nearly nonexistent. Lists of some of the hypersonic research to date are given in References 27 and 33.

Today the research in hypersonics is mainly being conducted in the growing field of computational fluid dynamics (CFD). This was made possible by the tremendous increases in the memory and computational power of modern supercomputers. It is now possible to obtain the complete three-dimensional inviscid flow field around a hypersonic vehicle. CFD has the advantages of being able to yield detailed pictures of the flow fields uncontaminated by intrusive measuring devices which disturb the flow. The large expense of experimental work makes CFD more attractive

for most universities. The CFD computer codes, however are only approximations of the physics of the flow and require simplifying assumptions to keep memory requirements and computational times reasonable even with the most powerful supercomputers. There are some experimental facilities still being used however. In order to initially validate the CFD methods, experimental results must be used. This is the only way to check the validity of the computational results when dealing with the real gas effects of hypersonic flows.

SIGNIFICANCE OF THE PROBLEM

In 1984, the interest in hypersonics was prompted by the need for more knowledge to support new vehicle concepts. Some of these projects are (37,2):

(1) The Aerodynamically Assisted Orbital Transfer Vehicle (AOTV), to be used to transfer payloads between geosynchronous orbit to low earth orbit (LEO) to a rendezvous with the shuttle. During the aerodynamic braking stage, the vehicle will travel hypersonically (Mach 36) through the earth's atmosphere at altitudes of 250,000 to 500,000 feet.

(2) The National Aerospace Plane (NASP). This Air Force vehicle will take off and land horizontally from conventional airports, be able to travel at Mach 12, go into orbit, deorbit and land. The civilian version of this vehicle will travel at about Mach 7 and about 150,000 feet. This is the so-called Orient Express Hypersonic Transport (OEST).

(3) A second-generation space shuttle. As technology and knowledge increase, a second-generation shuttle will need to be built to fulfill the need for a follow on space launch vehicle.

(4) Low-hypersonic missile anti-tank penetrators. The Army will use hypersonic (Mach 5-7), finestabilized, armor-piercing projectiles to penetrate advanced armors on future tanks and armored vehicles.

To help illustrate the challenge in studying hypersonic flow fields, consider a typical ICBM with a 5000 mile range. Such a vehicle reenters the atmosphere at Mach 20. At this speed the air temperature behind the normal shock from a blunt body can be as high as 6000K (10,740°F).

(17:341). At this temperature air no longer behaves as an ideal gas mixture of diatomic oxygen and nitrogen. Instead, it will dissociate and ionize. The resulting "real gas" will consist of monatomic and ionic oxygen, nitrogen, oxides of nitrogen, and free electrons. As this real gas mixture travels back along the vehicle away from the stagnation point, it expands and cools. There may be some chemical recombination if the pressure is high enough. If not, the original mixture will be "frozen" at its original composition. These non-equilibrium effects cause a large departure from conventional aerodynamic and heat transfer theories. These effects must be fully understood and accounted for in the design stage for any hypersonic vehicle. The only way to study these effects is to duplicate the hypersonic flow conditions in the laboratory.

GROUND TEST FACILITIES

The experimental facilities used today for hypersonic research are of three basic types: continuous, blowdown, and impulse. Table 1 gives the characteristics of each type. Conventional experimental tools for getting aeronautical information, such as supersonic wind tunnels, are inadequate for investigating the real gas effects of the flow around vehicles at hypersonic speeds because of the reservoir temperature limitations. An impulse facility (shock tubes, shock tunnels, and gun tunnels) is the only facility that can exactly duplicate hypersonic flow conditions. For this reason some researchers continue to use shock tunnels for experimental hypersonic research. (For an excellent description on the operation of hypersonic shock tunnels see Reference 30.) Figure 1 gives a good description of the test times and maximum stagnation temperatures attainable in the various ground test facilities. Since the flow duration in a shock tunnel is between 1 and 10 milliseconds (ms), it is imperative that the conditions be optimized for each run to obtain the maximum test time possible. Note that a test time of one millisecond is not as limiting as it may sound. The response times of pressure transducers and thin film heat gauges are on the order of a microsecond. In order to aid the experimenter in determining the best possible test times in a hypersonic shock tunnel, CFD can be used to model the starting process in the shock tube and the flow processes in the hypersonic nozzle and test section. This is easier and can yield more accurate results than running several sets of conditions in the shock tunnel to determine the best test times.

	Continuous Flow	Blow Down	Impulse
Mach No.	1.5 to 10	1.4 - 14	7 - 86
Run Time	continuous	seconds to minutes	1 - 100 ms
Test Time	long	medium	short
Repeatability	excellent	medium	low
Cost	very high	high	low
Stagnation Temperature T ₀	low	low	high
Set-up Time	very long	short	short
Reynolds No.	low	medium	high
Instrumentation	standard	standard	special
Productivity	very high	medium	low

TABLE 1. Comparison of test facilities (45:7,8,10).

The test time (flow duration time) in a hypersonic shock tunnel is limited by the starting process in the nozzle, and the passage of either the reflected shock from the shock-contact surface intersection or the reflected head of the expansion wave from the shock tunnel driver section (30:--; 40:--). The aim of the experimenter is to achieve the maximum possible flow duration time with a high enough stagnation temperature (high incident shock Mach number) to duplicate hypersonic reentry. A sample wave diagram is shown in Figure 2 to show the significance of the test time.

The shock tunnel produces a strong shock wave by the rupture of the diaphragm. This shock wave travels down the driven tube until it partially reflects off the nozzle shoulders and travels toward the driver section. The shock also travels into the nozzle starting the flow. In the nozzle, this starting shock is followed by a contact surface and a rearward facing shock that is "swallowed" by the high velocity gas flow in the nozzle. Testing can commence once this swallowed shock clears the test section (40:2).

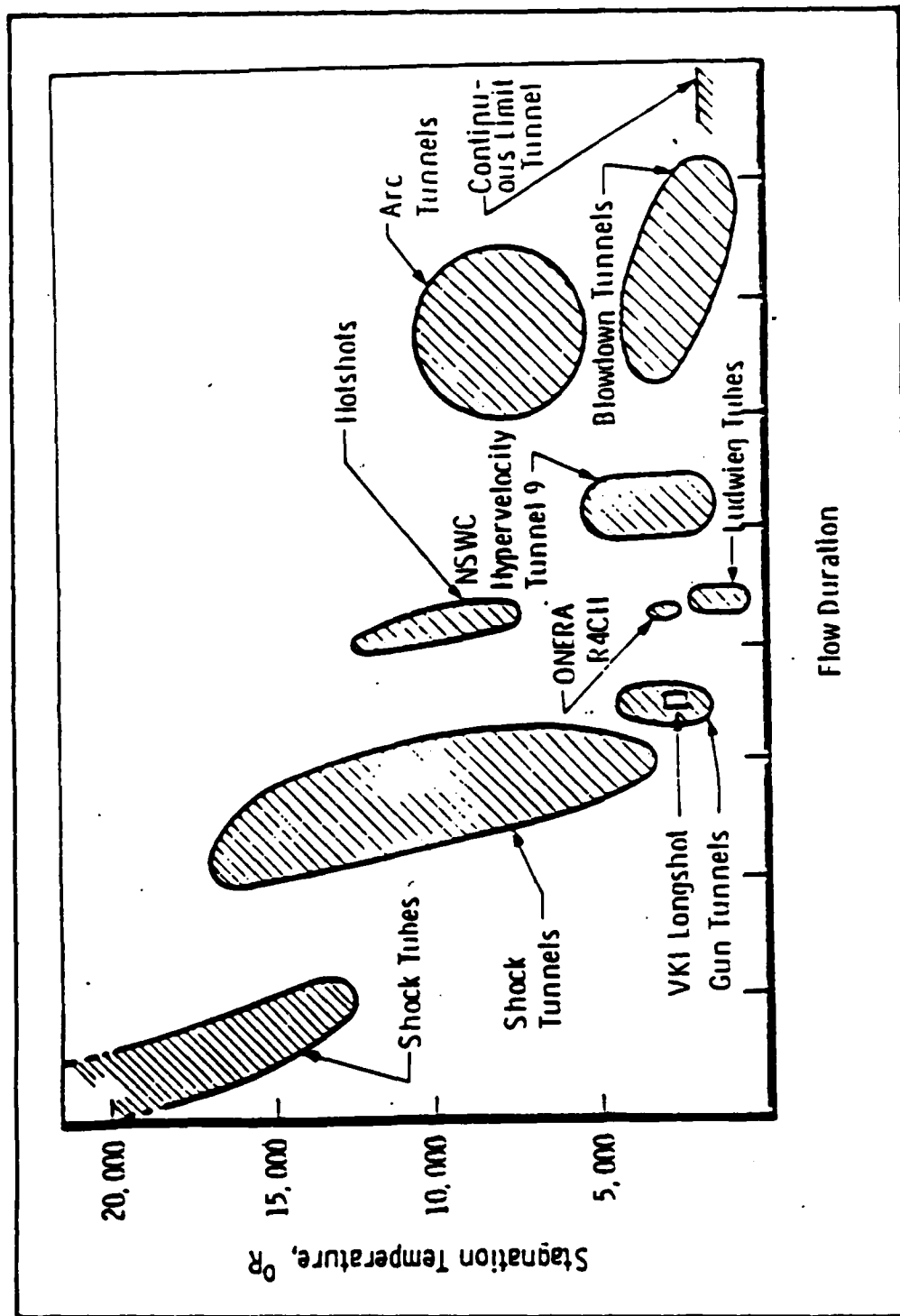


Figure 1. Stagnation temperature and flow duration time for test facilities (45; Figure 6).

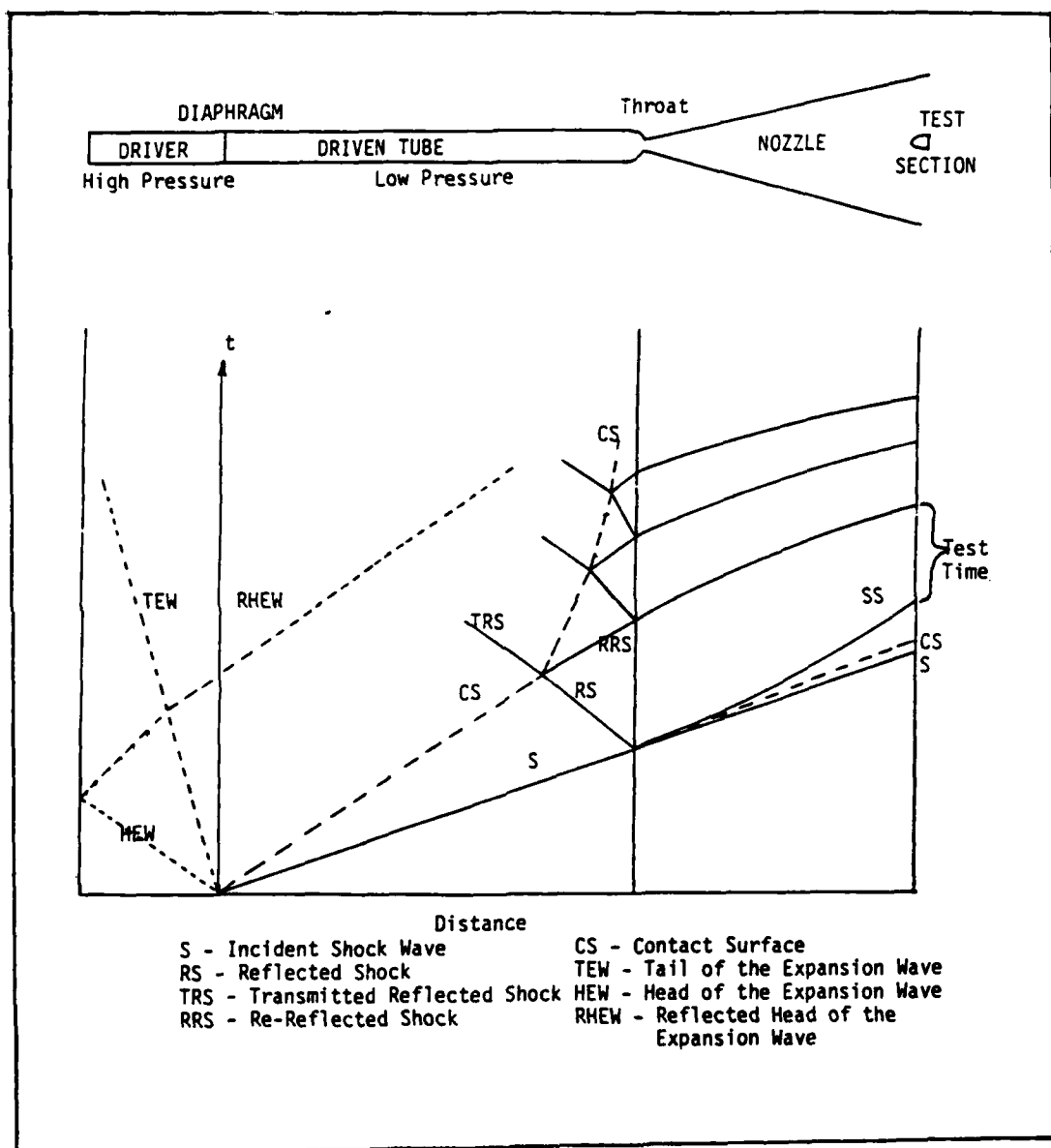


Figure 2. Typical wave diagram for a hypersonic shock tunnel.

In the most common case occurring in a shock tunnel, the reflected shock eventually intersects the approaching contact surface. For most cases this intersection produces two shocks, one that is transmitted through the contact surface toward the driver, and a reflected shock that travels back toward the nozzle. The reflected shock then partially reflects off the nozzle shoulders and intersects the contact surface again. It also continues into the nozzle where it ends testing when it disturbs the flow conditions in the nozzle (45:4). Two other cases may occur. One is the unsteady expansion head may reflect off the driver end wall, overtake the contact surface and travel into the nozzle. This ends the test time before any shock wave-contact surface intersection can take place. This is more common with very short drivers, gases with high acoustic velocity in the driver (such as helium or hydrogen), and very low shock Mach numbers. The other case occurs if a gas with a high acoustic speed is used in the driver (helium, hydrogen or hydrogen/oxygen combustion drivers). This will produce a "soft" contact surface (4:446-447). When the reflected shock intersects this soft contact surface it produces a transmitted shock but instead of a reflected shock a reflected expansion is produced. The head of this expansion travels into the nozzle at the local fluid velocity plus the local speed of sound.

Chapter Two

NUMERICAL METHODS FOR HYPERSONIC FLOW

ASSUMPTIONS AND LIMITATIONS

Two major factors in choosing a numerical method were the computing power available and the applicability of a particular scheme. The computer used for this study was a Prime 850 minicomputer--a relatively slow machine with virtual memory architecture. The code was kept simple to preclude excessive computing times. This was the major reason for rejecting the CFD methods which account for fluid viscosity and real gas effects. Computing was also limited to one-dimensional where possible. The only place in the shock tunnel where two-dimensional computations were done was in the nozzle section where strong two-dimensional effects were found. A look at the literature shows some numerical work centered mainly on the nozzle starting process but not on the entire shock tunnel operation (40:2). An excellent text on CFD is Reference 1. This gives several numerical methods that are applicable for hypersonic flow and this study. Reference 40 describes previous work on the nozzle starting process, while Reference 15 describes the propagation of a shock through the nozzle. The computer code used in Reference 40 was a good first-order scheme but was found unsuitable for this study due to its tendency to smear the shocks somewhat and the contact surfaces greatly.

DESCRIPTION OF NUMERICAL METHOD USED

One of the most critical interactions affecting the test times in hypersonic shock tunnels is the interaction of the reflected shock and the contact surface. If the contact surface is not properly treated, inaccurate estimates of the test time could result. For this reason a numerical method which has good performance in treating contact surfaces was sought. Such a method was developed and refined by Harten (10:--) and written into a computer code for this study by Carafano (28:--). The Harten method does not smear the contact surface like the first order methods such as Godunov, Roe, or Lax. It also does not have the instability

problem near severe discontinuities like the second-order methods of MacCormack, Lax-Wendroff, and others. For these reasons the Harten method described in References 10 and 28 was chosen for this study.

The Harten method is a second-order accurate numerical scheme which solves the unsteady compressible Euler equations, the continuity equation, and the energy equation. The code as written treats the fluids as perfect gases with no viscosity (28:13-15). The code takes into account two separate gases--one for the driver and one for the test gas. Thus the code can handle helium driven shock tunnels as well as combustion driven tunnels. However, combustion driven shock tunnels should be handled with caution. Since the code only handles perfect gases, the maximum shock Mach number must be kept below about six to preclude the occurrence of real gas effects (dissociation and ionization) caused by the very high stagnation temperatures.

The code treats the shock tube portion of the calculations as strictly one-dimensional. The hypersonic nozzle can be treated as either one-dimensional or two-dimensional axi-symmetric. Graphics packages were written that produce: two-dimensional contour plots of the flow in the nozzle, history plots of thermodynamic properties, and distributions of pressure and Mach number in the shock tube.

The RPI shock tunnel modeled in this study is shown in Figure 3. An enlargement of the nozzle area is shown in Figure 4. The transducer locations are shown. These allow histories to be made of the state variables. Table 2 shows the exact transducer locations as measured from the driver end wall. The Mach number shown is the Mach number at that location with fully developed steady flow.

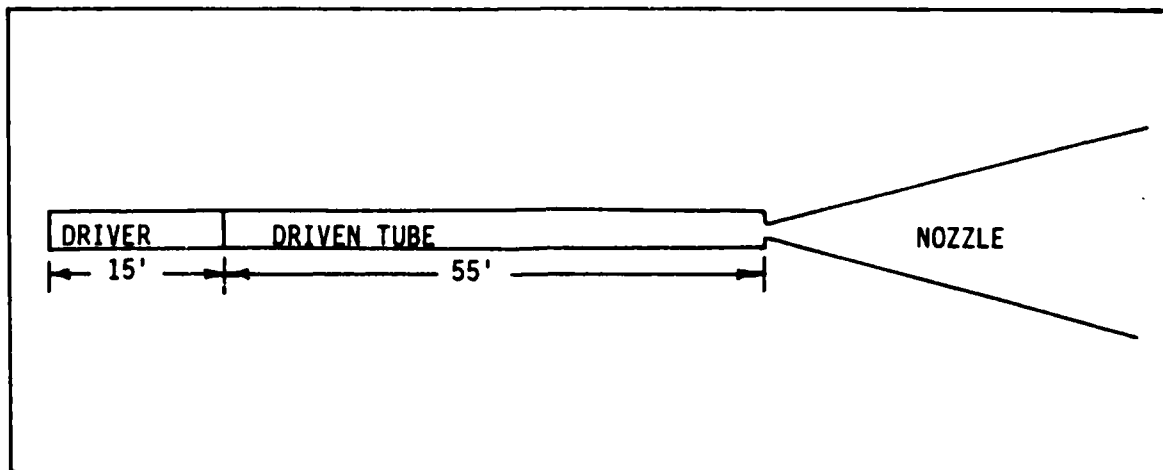


Figure 3. RPI shock tunnel layout.

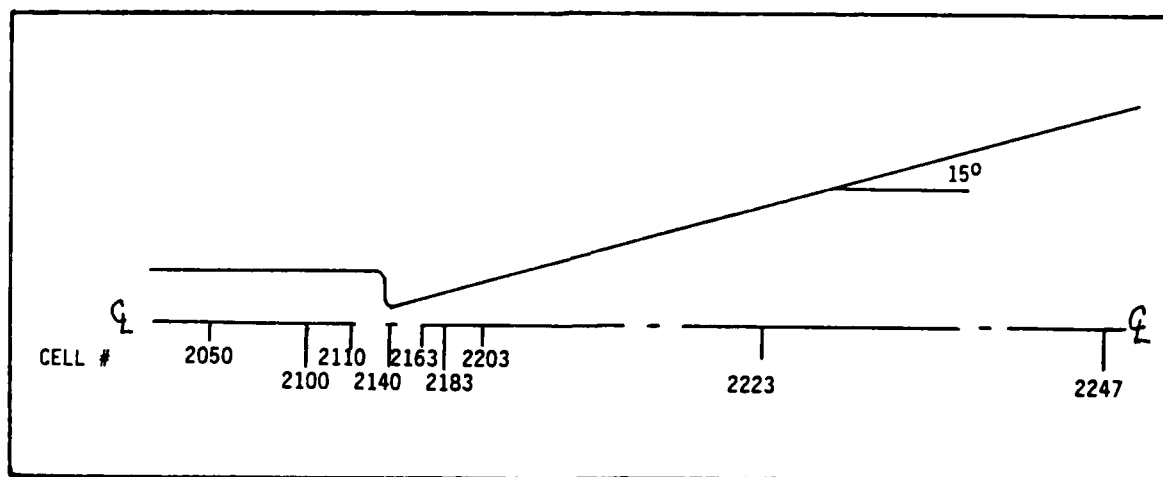


Figure 4. Nozzle section layout and transducer locations.

<u>Cell Position</u>	<u>X Position</u> <u>(Inches)</u>	<u>Radius</u> <u>(Inches)</u>	<u>A/A*</u>	<u>Mach No.</u>
1900	810.3	2.0	16.	0.03
1950	820.	2.0	16.	0.03
2000	829.3	2.0	16.	0.03
2050	838.3	2.0	16.	0.03
2100	847.	2.0	16.	0.03
2110	848.5	2.0	16.	0.03
2140	850.9	0.5	1.	1.0
2163	852.6	0.847	2.87	2.59
2183	855.4	1.6	10.3	3.95
2203	860.7	3.0	36.6	5.5
2223	870.7	5.7	129.4	7.4
2247	894.7	12.1	587.3	10.

Table 2. Shock tunnel transducer data.

Chapter Three

DISCUSSION AND ANALYSIS OF NUMERICAL DATA

MACH 2.3 INCIDENT SHOCK

Air Driver

The first set of results are those for an air driven shock of Mach 2.3. The stagnation temperature obtained for this Mach number is 1200°F. Other Mach numbers and stagnation temperatures are shown in Table 3.

<u>Incident Mach No.</u>	<u>To(F)</u>
2.3	1200
3.41	2700
5.4	6900

Table 3. Stagnation temperature and shock Mach number.

The static pressure history at the exit of the nozzle is shown in Figure 5. The top trace corresponds to the Mach 10 flow conditions at the exit of the nozzle and the bottom trace is at the Mach 7.4 position inside the nozzle. The ordinate is the pressure and the abscissa is the time in ms since diaphragm rupture. The three numbers in parentheses to the left of each curve are the transducer cell x location, y location and the full scale value of the plot. All thermodynamic properties are nondimensionalized with respect to the dump tank values.

At the exit of the nozzle the starting shock wave is seen as a rapid rise in pressure. The rearward or "swallowed" shock is seen as the rapidly falling pressure. The resulting steady low pressure is the test pressure at the exit of the nozzle indicating fully developed Mach 10 flow conditions. These conditions start at about 23.75 ms.

and at about 31.25 ms a rise is visible in the pressure trace. This is the shock wave that has reflected off the nozzle shoulders, then off the contact surface, and traveled through the nozzle disturbing the flow conditions and ending the test conditions. The total test time for this case is about 7.5 ms. A plot of density and probe total pressure are shown in Figures 6 and 7 respectively. Additional flow details can be seen in these plots as well as the very well-defined steady state test conditions.

The termination of the test time for this case was caused by the arrival of a shock wave which originated with the incident shock from the initial diaphragm rupture. This

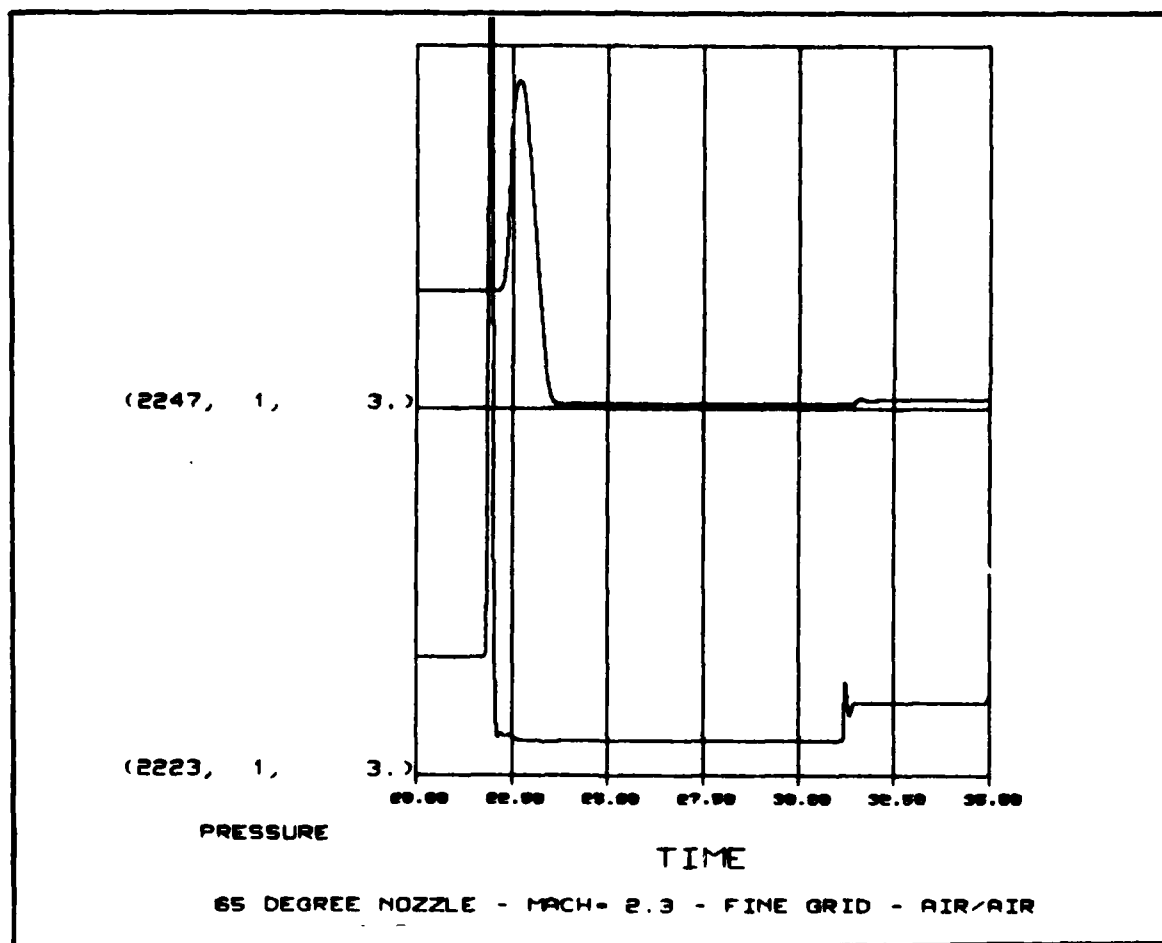


Figure 5. Static pressure history Mach 10 (upper) and Mach 7.4 (lower). Mach 2.3 incident shock, air driver.

shock traveled down the tube, ruptured the nozzle diaphragm, reflected off the nozzle shoulders, traveled back upstream toward the driver end of the tube, reflected off the contact surface and then traveled through the nozzle to the test section. Each time the shock hits the shoulders of the nozzle a transmitted wave travels down the nozzle and a reflected wave travels toward the driver. Also, each time a shock wave encounters the contact surface, a transmitted wave travels toward the driver and a reflected wave travels toward the nozzle. This complicated wave pattern is sketched in Figure 2. The first reflected wave is the only one of interest in this study since it is responsible for

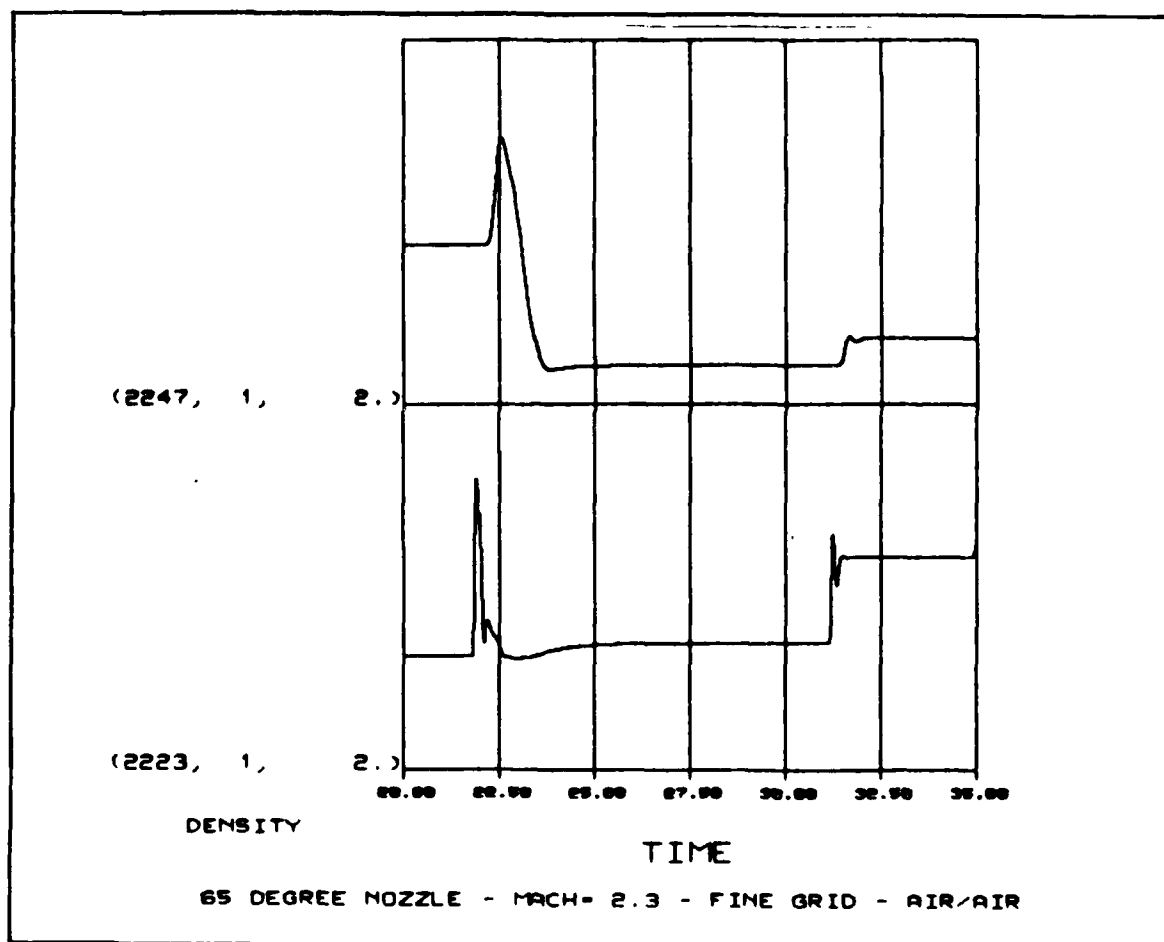


Figure 6. Density history Mach 10 (upper) and Mach 7.4 (lower). Mach 2.3 incident shock, air driver.

ending the test conditions in the nozzle.

Another look at the shock-contact surface interactions can be done with a pressure and Mach number versus distance plot as shown in Figure 8. This is a discrete plot of static pressure and local Mach number distribution along the tube. Figure 8 shows the distribution 14 ms after diaphragm rupture. The incident shock wave can be seen at location 635. At location 494, the contact surface is visible only in the Mach number plot, since the pressure is equal across a contact surface. The unsteady expansion can be seen from about location 352 to the driver end wall.

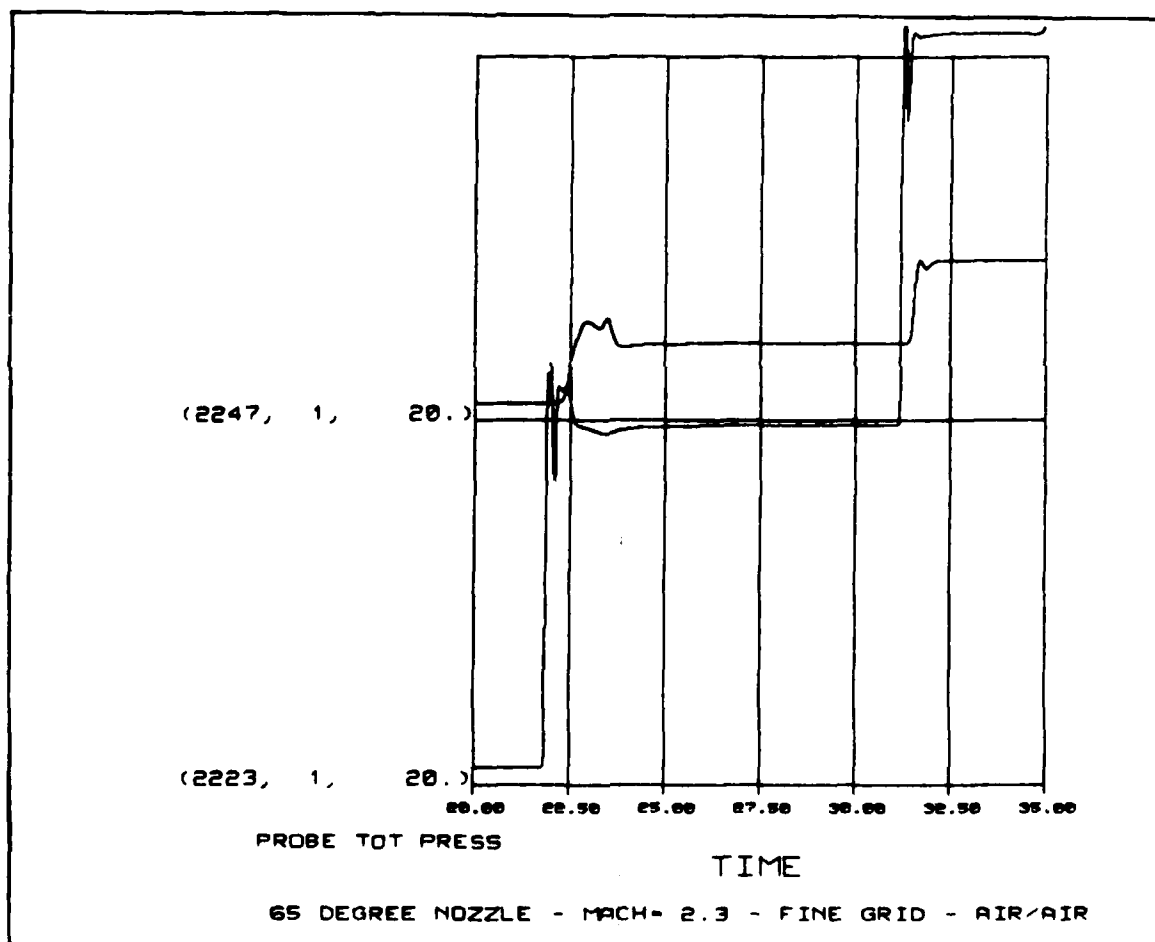


Figure 7. Probe total pressure history Mach 10 (upper) and Mach 7.4 (lower). Mach 2.3 incident shock, air driver.

Figure 9 shows the same plot at a later time, 21 ms. The shock has just ruptured the nozzle diaphragm at location 847. The contact surface and expansion are evident. It is clear from the two plots that the contact surface is moving away from the unsteady expansion which will result in the shock reflecting off the nozzle shoulders and encountering the contact surface and not the expansion. Figure 10 shows this about to happen. Notice that the shock has reflected off the nozzle shoulder and is traveling toward the contact surface. The reflected shock is evident from the high pressure region at the right side of the plot. In Figure 11 the shock has intersected the contact surface and resulted in a reflected shock which traveled into the nozzle.

In order to maximize test conditions in a fixed geometry shock tunnel, the reflected shock from the contact surface interaction must be eliminated. The subject of shock wave contact surface interaction is treated very well in several texts (5:--; 6:417-423). This can be accomplished by matching the acoustic impedance of the gases on either side of the contact surface. In the RPI tunnel this can be done

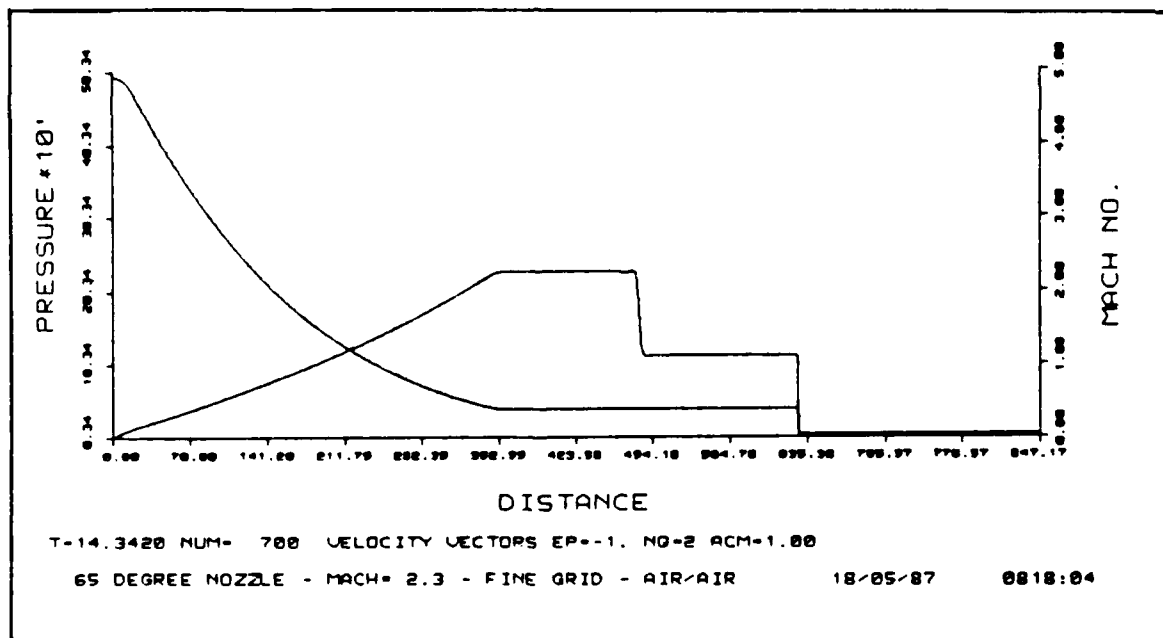


Figure 8. Mach number and pressure distribution, 14.3 ms.
Mach 2.3 shock, air driver.

by using helium as the driver gas and operating at the required Mach number to achieve this "tailored" contact surface. Using helium to create a tailored contact surface calls for an incident shock Mach number of 3.41. Before the results of the tailored case are presented, the results of using helium and a shock of 2.3 are presented.

Helium Driver

The pressure and Mach number versus distance plot for the helium driven Mach 2.3 case are shown at 28.5 ms in Figure 12. At this time the shock has already reflected off the nozzle shoulders. Notice the sloping traces near the right side of the plot. This indicates that the reflected head of the expansion has passed through the contact surface (visible at location 670) and has traveled into the nozzle. In this case the contact surface is "soft" and an expansion will result from the intersection of the shock and contact surface (6:420). The test time will end when the expansion moves into the nozzle.

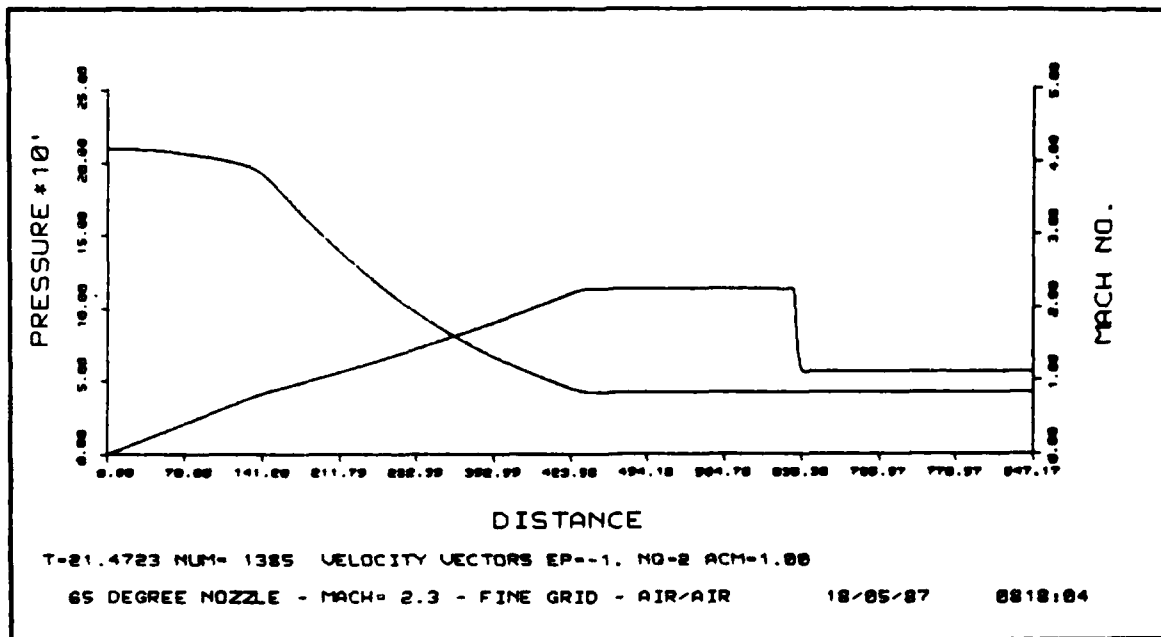


Figure 9. Mach number and pressure distribution, 21.5 ms.
 Mach 2.3 shock, air driver.

The total pressure history for this case is shown in Figure 13. Notice at the exit of the nozzle, flow conditions last only about 0.5 ms. This is much shorter than the results obtained with the air driver. This is due to the acoustic velocity of the helium being about four times faster than that of air. This causes the reflected head of the expansion wave to close on the shock wave, thereby cutting test time. Also the reflected shock-contact surface intersection yields a reflected expansion which moves into the nozzle further reducing test time. This type of shock-contact surface interaction is shown in Figure 14(e). Therefore, for low Mach numbers, air is a better choice for a driver gas with this tube layout.

MACH 3.41 INCIDENT SHOCK

Using room temperature gases, a helium driver and air test gas can produce a tailored contact surface if a Mach 3.41 incident shock is used (5:353). With this setup a reflected shock will not occur when a shock encounters the contact surface. These flow conditions were run and can be

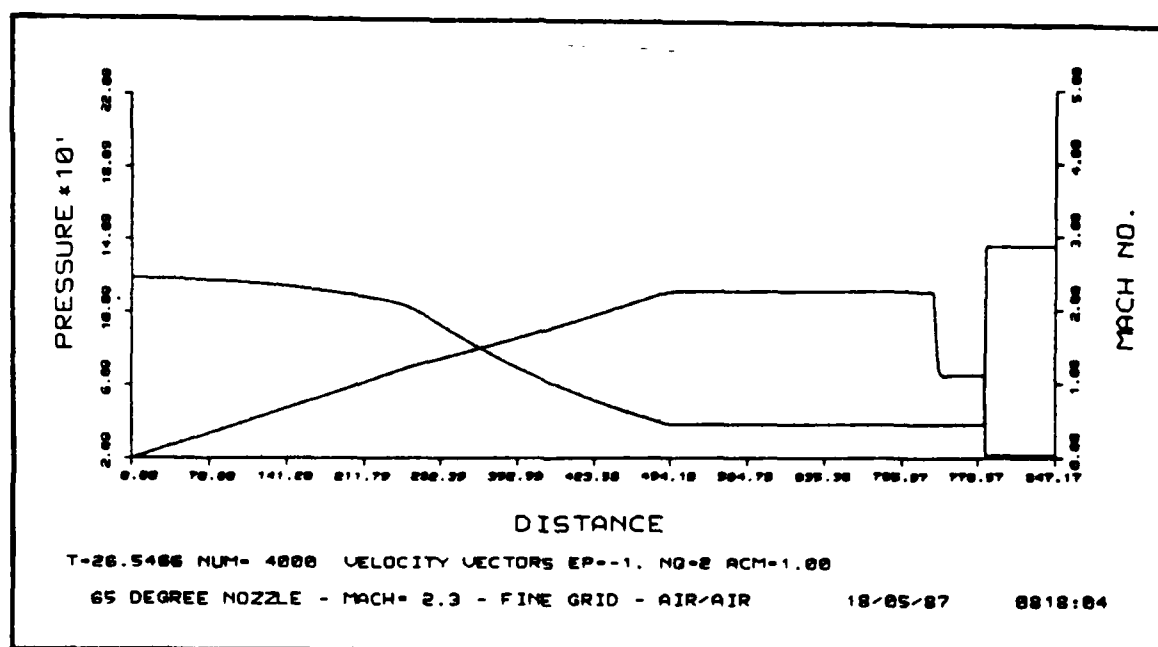


Figure 10. Mach number and pressure distribution, 26 ms.
 Mach 2.3 shock, air driver.

seen in the next set of figures. The distribution plot is shown for this case in Figure 15. The shock has already reflected off the nozzle shoulders, has passed through the contact surface without reflecting and is traveling toward the driver end wall. The sloping pressure curve to the right of the shock show the expansion wave already passing through the shock and traveling toward the nozzle. Figure 16 shows the probe total pressure at the exit of the nozzle. Notice the arrival of the starting shock by the rapid rise in the pressure in the test section, the "swallowed" or rearward facing shock by the sharp drop in pressure to the steady state test conditions. The test conditions terminate with the arrival of the reflected expansion which is clearly seen as the unsteady decrease in pressure. This case resulted in 4 ms test time. This would not have been possible with air as the driver gas.

MACH 5.4 INCIDENT SHOCK

For the last case of this study, a Mach 5.4 incident shock corresponding to 6900°F stagnation temperature was used. At these conditions, the contact surface will no

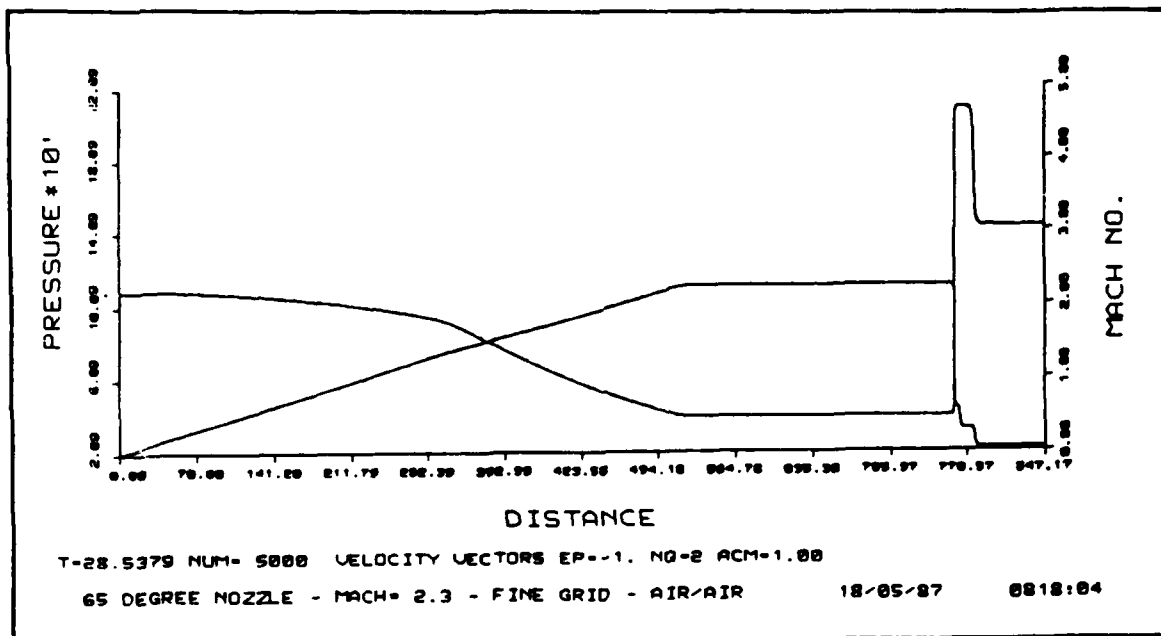


Figure 11. Mach number and pressure distribution, 28 ms.
Mach 2.3 shock, air driver.

longer be tailored and a "hard" reflection will occur such as that seen in the air driven case for Mach 2.3. Figure 17 shows the pressure at the last two transducer locations. At the exit of the nozzle, the test conditions last for about 1.5 ms. These conditions are terminated by the arrival of the first reflected shock from the contact surface. The Mach 5.41 shock conditions are the closest to the Mach 10, 150,000 ft. cruise conditions of about 7000°F stagnation temperature.

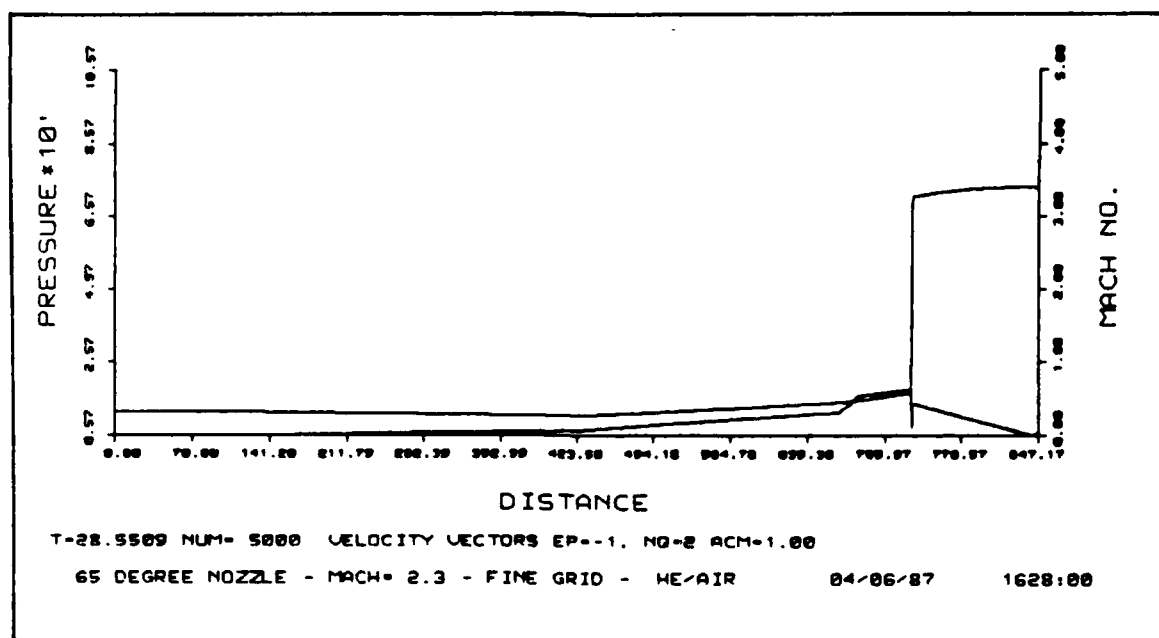


Figure 12. Mach number and pressure distribution, 28 ms.
Mach 2.3 shock, helium driver.

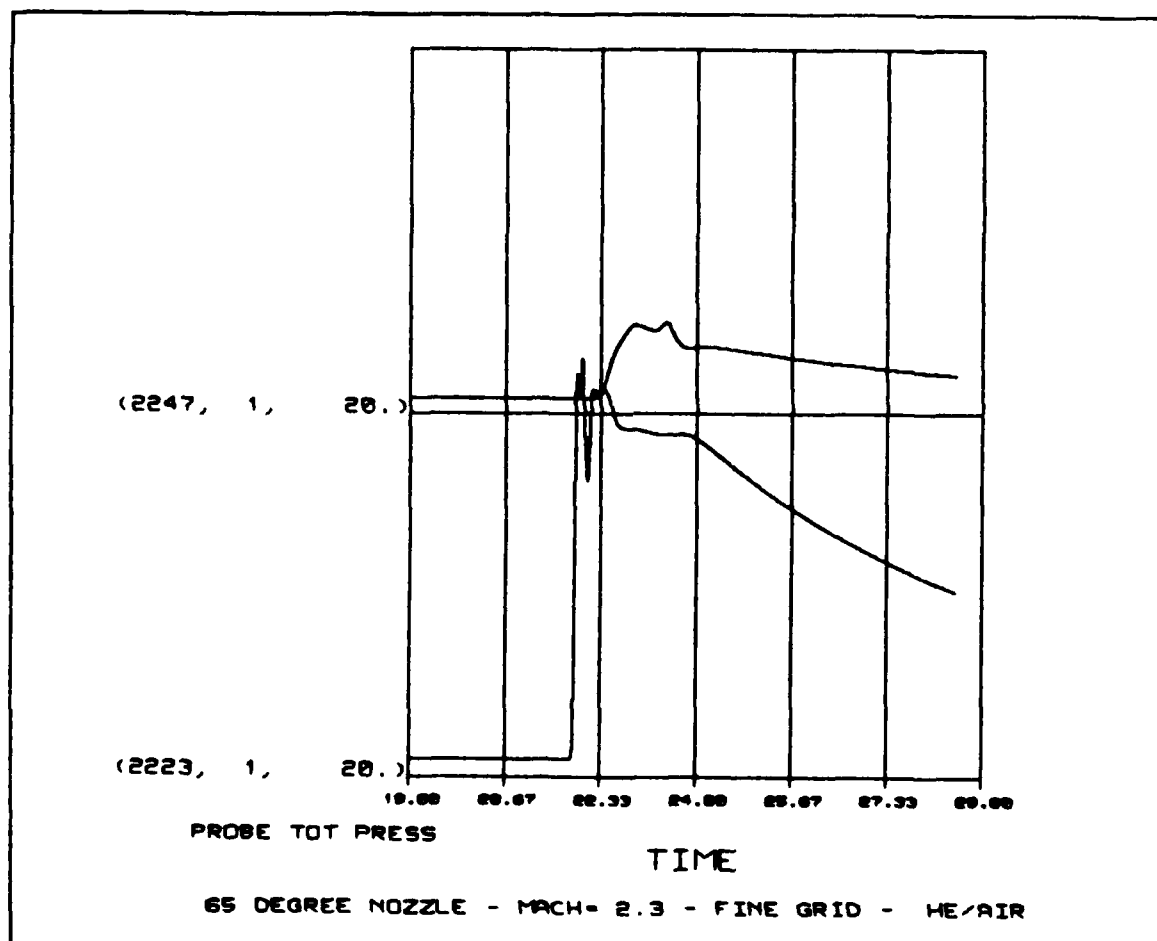


Figure 13. Probe total pressure history, Mach 10 (upper) and Mach 7.4 (lower). Mach 2.3 incident shock, helium driver.

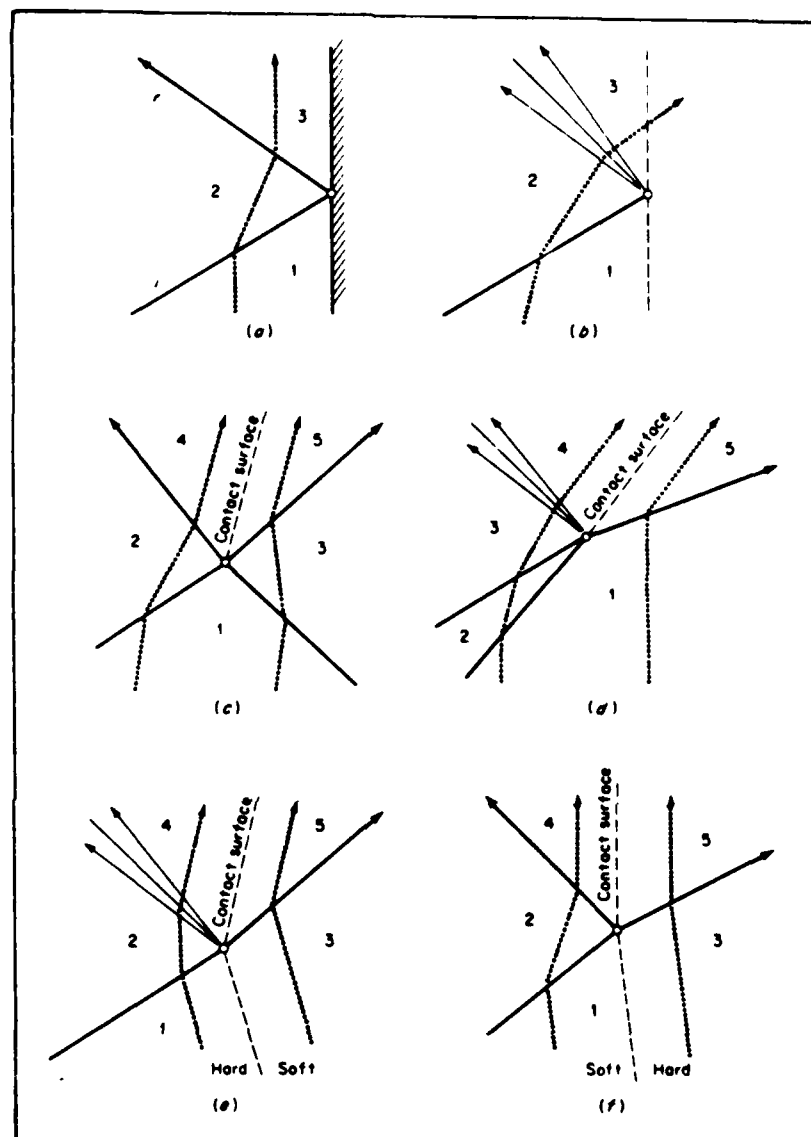


Figure 14. Wave diagram for shock interactions: (a) shock reflection from a rigid wall or closed end; (b) shock incident on open end at constant pressure; (c) intersection of shocks of opposite family; (d) intersection of shocks of common family; (e) shock incident on contact surface; and (f) shock incident on contact surface (6: Figure 8.35).

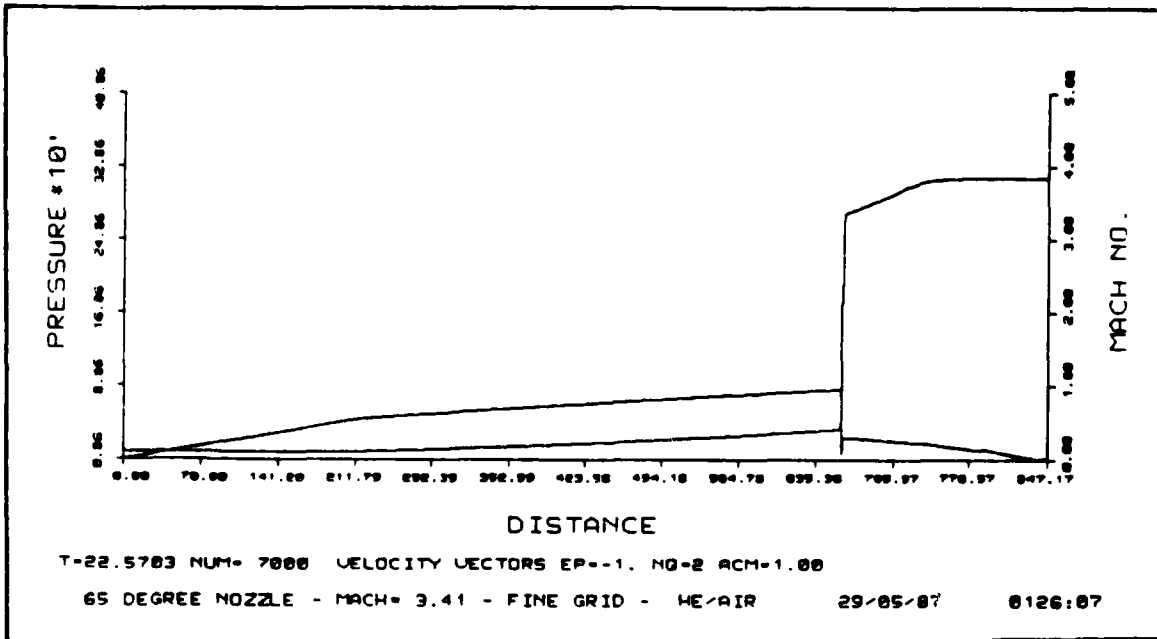


Figure 15. Mach number and pressure distribution, 22 ms.
 Mach 3.41 shock, helium driver.

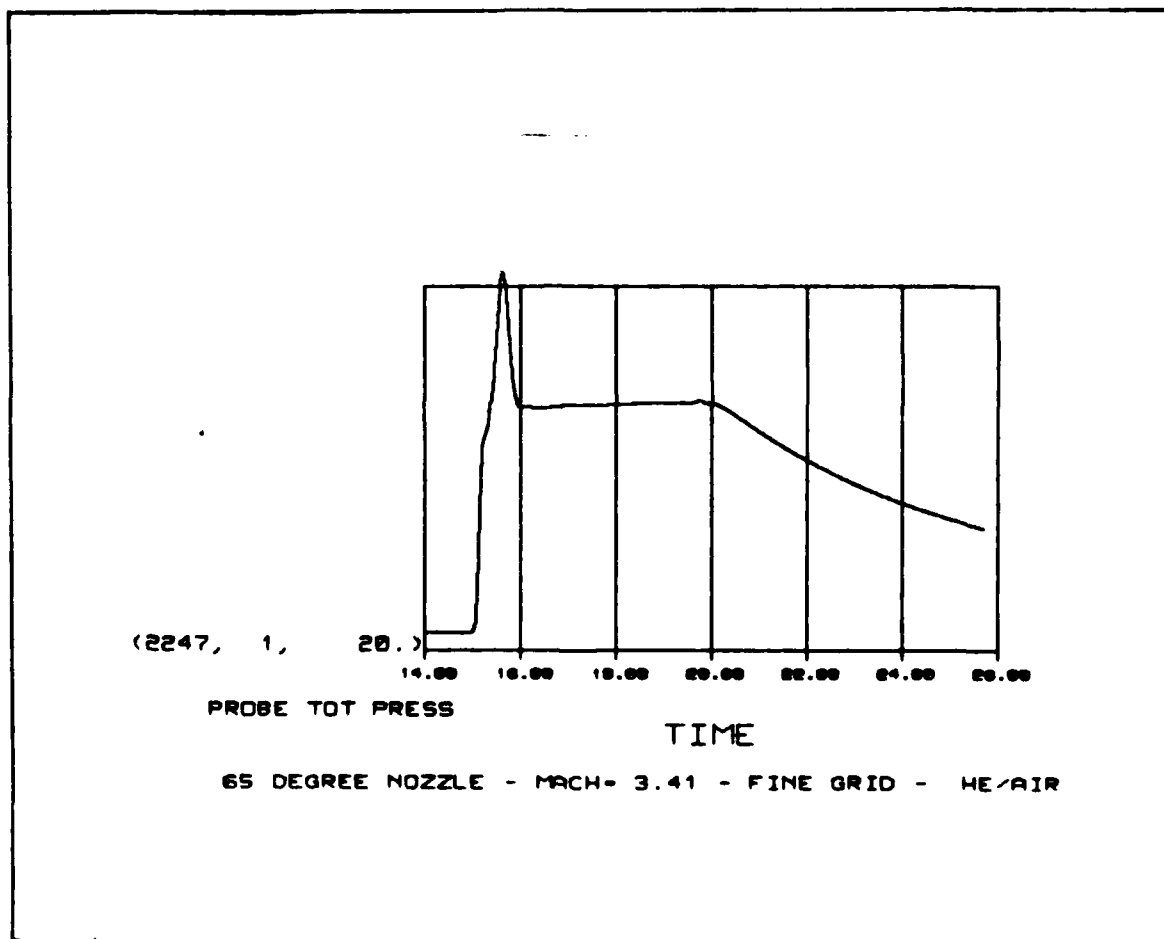


Figure 16. Probe total pressure history Mach 10. Mach 3.41 incident shock.

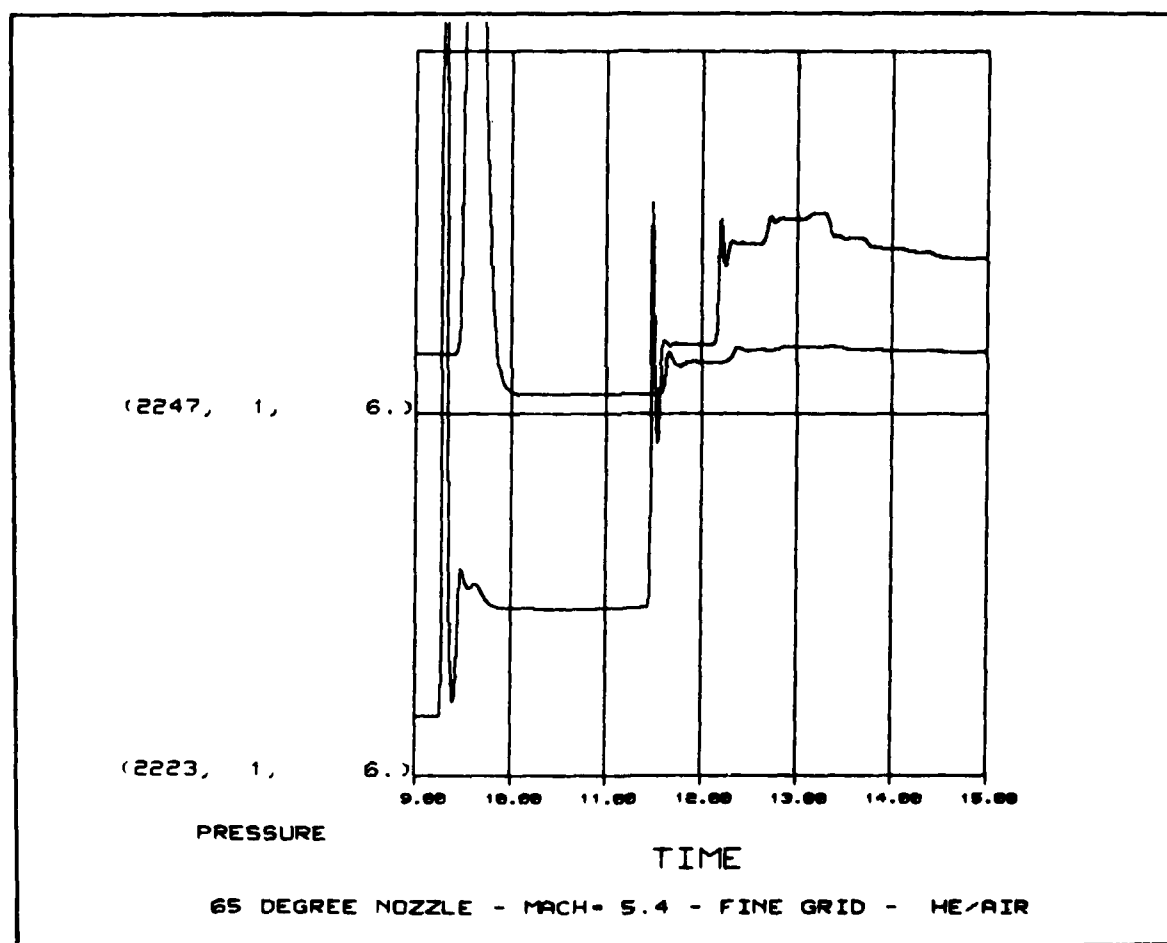


Figure 17. Static pressure history Mach 10 (upper) and Mach 7.4 (lower). Mach 5.4 incident shock.

Chapter Four

CONCLUSIONS

The numerical scheme, Harten's Total Variational Diminishing (TVD), adapted for this problem by Carofano (28:--), accurately modeled the unsteady, compressible flow of a shock tunnel. The TVD scheme also accurately modeled the nozzle starting process to include the transversal by the starting shock, the formation and passage of the contact surface and the rearward facing shock. The TVD scheme also accurately modeled the shock wave/contact surface intersection problem.

Accurate estimates of the total available test time for the RPI hypersonic shock tunnel were obtained. The maximum test time occurred for the Mach 2.3 incident shock with air as the driver gas. This time was found to be 7.5 ms. For higher stagnation temperatures, and hence higher incident shock Mach numbers, helium is needed as the driver gas. Under these conditions, the maximum test time was found to occur at the tailored contact surface condition or Mach 3.41. The test time at this condition was 4 ms. The maximum test time occurred with air as the driver gas and low shock Mach numbers.

At the highest Mach number studied, Mach 5.4, the test time was found to be 1.5 ms. This is certainly long enough to obtain valuable data with the fast response time of modern instrumentation and signal processing techniques.

<u>Mach No.</u>	<u>Test Time (ms)</u>	<u>Driver Gas</u>
2.3	7.5	Air
2.3	0.5	Helium
3.41	4.0	Helium
5.4	1.5	Helium

Table 4. Comparison of Test Times.

RECOMMENDATIONS

Viscous effects need to be studied. The test times can be affected by the formation of boundary layers and other viscous effects and hence need to be modeled.

Adaptive grid techniques need to be employed to keep computation times down and to obtain higher resolution. The present study with a fixed grid and mostly one-dimensional computations took an enormous amount of computer time to solve the equations within acceptable limits. On the order of 30-45 CPU hours were used per set of conditions.

Lastly, and most important, experiments need to be run which duplicate the numerical simulations. This will allow a good comparison to be made between experimental and numerical results to determine the effectiveness of the present code.

BIBLIOGRAPHY

Books

1. Anderson, D.A., Tannehill, J.C. and Fletcher, R.H. Computational Fluid Mechanics and Heat Transfer. New York: McGraw Hill Book Co., 1984.
2. Cox, R.N. and Crabtree, L.F. Elements of Hypersonic Aerodynamics. New York: Academic Press, 1965.
3. Dorrance, W.H. Viscous Hypersonic Flow. New York: McGraw Hill Book Co., 1962.
4. Hays, W.D. and Probstein, R.F. Hypersonic Flow Theory, Second Edition, Volume I, Inviscid Flow. New York: Academic Press, 1966.
5. Owczaryk, J. Fundamentals of Gas Dynamics. Scranton, PA: International Textbook Co., 1964.
6. Thompson, P.A. Compressible Fluid Dynamics. New York: McGraw Hill Book Co., 1972.

Articles and Periodicals

7. Anderson, G.Y., Bencze, D.P. and Sanders, B.W. "Ground Tests Confirm the Promise of Hypersonic Propulsion." Aerospace America, Vol. 25, No. 9 (September 1987), pp. 38-42.
8. Camm, J.C. and Rose, P.H. "Electric Arc-Driven Shock Tube." The Physics of Fluids, Vol. 6, No. 5 (May 1963), pp. 663-678.
9. Colladay, R.S. "Rekindled Vision of Hypersonic Flight." Aerospace America, Vol. 25, No. 8 (August 1987), pp. 30-31, 34.
10. Harten, A. "High Resolution Schemes for Hyperbolic Conservation Laws." Journal of Computational Physics, Vol. 49 (1983), pp. 357-393.

11. Hindeman, R.G. "Generalized Coordinate Forms of Governing Fluid Equations and Associated Geometrically Induced Errors." AIAA Journal, Vol. 20, No. 10 (1982), pp. 1359-1367.
12. Jackson, L.R., et. al. "Hypersonic Structures and Materials: A Progress Report." Aerospace America, Vol. 25, No. 10 (October 1987), pp. 24-30.
13. Johnston, P.J., et. al., "Fitting Aerodynamics and Propulsion into the Puzzle." Aerospace America, Vol. 25, No. 9 (September 1987), pp. 32-34, 37, 42.
14. Jones, R.A. and Donalson, C.D. "From Earth to Orbit in a Single Stage." Aerospace America, Vol. 25, No. 8 (August 1987), pp. 32-34.
15. Kashimura, H., Iwata, N. and Nishida, M. "Numerical Analysis of the Wave Propagation in a Duct." JSME, Vol. 29, No. 251 (May 1986), pp. 1-6.
16. Li, T.Y. and Nagamatsu, H.T. "Shock Wave Effects on the Laminar Skin Friction of an Insulated Flat Plate at Hypersonic Speeds." Journal of Aeronautical Sciences, Vol. 20 (May 1953), pp. 345-355.
17. Nagamatsu, H.T., Geiger, R.E. and Sheer, R.E., Jr. "Real Gas Effects in Flow Over Blunt Bodies at Hypersonic Speeds." Journal of the Aerospace Sciences, Vol. 27, No. 4 (April 1960), pp. 241-251.
18. Nagamatsu, H.T. and Sheer, R.E., Jr. "Boundary Layer Transition on a 10° Cone in Hypersonic Flows." AIAA Journal, Vol. 3, No. 11 (November 1965), pp. 2054-2061.
19. Nagamatsu, H.T. and Sheer, R.E., Jr. "Hypersonic Shock Wave-Boundary Layer Interaction and Leading Edge Slip." ARS Journal, Vol. 30 (May 1960), pp. 454-462.
20. Nagamatsu, H.T. and Sheer, R.E., Jr. "Vibrational Relaxation and Recombination of Nitrogen and Air in Hypersonic Nozzle Flows." AIAA Journal, Vol. 3, No. 8 (August 1965), pp. 1386-1391.
21. Nagamatsu, H.T., Sheer, R.E., Jr. and Graber, B.C. "Hypersonic Laminar Boundary Layer Transition on 3-Foot-Long, 10° Cone, $M=9.1-16$." AIAA Journal, Vol. 5, No. 7 (July 1967), pp. 1245-1251.

22. Nagamatsu, R.E., Sheer, R.E., Jr. and Schmid, J.R.
"High Temperature Rarefied Hypersonic Flow Over a
Flat Plate." ARS Journal, Vol. 31 (July 1961), pp.
902-910.
23. Nagamatsu, R.E., Weil, J.A. and Sheer, R.E., Jr. "Heat
Transfer to Flat Plate in High Temperature Rarefied
Ultrahigh Mach Number Flow." ARS Journal, Vol. 32
(April 1962), pp. 533-541.
24. Nagamatsu, H.T., Workman, J.B. and Sheer, R.E., Jr.
"Hypersonic Nozzle Expansion of Air with Atom
Recombination Present." Journal of the Aerospace
Sciences, Vol. 28, No. 11 (November 1961), pp.
833-837.
25. Nagamatsu, H.T., Workman, J.B. and Sheer, R.E., Jr.
"Oblique Shock Relations for Air at Mach 7.8 and
7200°R Stagnation Temperature." ARS Journal, Vol.
30 (1960), pp. 619-623.

Papers and Reports

26. Alpher, R.A. and White, D.R. "Ideal Theory of Shock
Tubes with Area Change Near Diaphragm." General
Electric Co. Report No. 57-RL-1664, Schenectady,
New York, 1957.
27. Anderson, J.D., Jr. "A Survey of Modern Research in
Hypersonic Aerodynamics." AIAA Paper 84-1578
presented at the AIAA 17th Fluid Dynamics, Plasma
Dynamics and Lasers Conference. Snowmass,
Colorado, June 25-27, 1984.
28. Carofano, G.C. "Blast Computation Using Harten's Total
Variation Diminishing Scheme." US Army Armament
Research and Engineering Center Report. Watervliet,
New York, 1987.
29. Li, T.Y. and Nagamatsu, H.T. "Hypersonic Viscous Flow
on Noninsulated Flat Plate." Proceedings of the
4th Midwestern Conference of Fluid Mechanics.
Purdue University, No. 128, (1955) pp. 273-287.
30. Nagamatsu, H.T. "Shock Tube Technology and Design."
General Electric Co. Report No. 58-RL-2107,
Schenectady, New York, 1958.

31. Nagamatsu, H.T., Graber, B.C. and Sheer, R.E., Jr.
"Laminar Cone Boundary Layer Transition $M=10.2$ to 13.8 ," General Electric Co. Report No. 65-C-005, Schenectady, New York, 1965.
32. Nagamatsu, H.T., Pettit, W.T. and Sheer, R.E., Jr.
"Heat Transfer on a Flat Plate in Continuum to Rarefied Hypersonic Flows at Mach Numbers of 19.2 and 25.4." NASA Contract Report NASA CR-1692, Washington, D.C., 1970.
33. Nagamatsu, H.T. and Sheer, R.E., Jr. "Hypersonic Gas Dynamics." Paper 85-0999 presented at the AIAA 20th Thermophysics Conference. Williamsburgh, VA, June 19-21 1985.
34. Nagamatsu, H.T. and Sheer, R.E., Jr. "Sharp Flat Plate Heat Transfer in Helium at Mach Numbers of 22.8 to 36.8." Paper 82-0295 presented at the AIAA 20th Aerospace Sciences Meeting. Orlando, FL, January 11-14, 1982.
35. Nagamatsu, H.T., Sheer, R.E., Jr. and Graber, B.C.
"Mechanics of Hypersonic Boundary Layer Transition on a Slender Cone." General Electric Co. Report No. 68-C-387, Schenectady, New York, 1968.
36. Nagamatsu, H.T., Sheer, R.E., Jr. and Weil, J.A.
"Improvements in Hypersonic Technique and Instrumentation." General Electric Co. Report No. 62-RL-3107C, Schenectady, New York, 1962.
37. Nagamatsu, H.T., Weil, J.A. and Sheer, R.E., Jr.
"Leading Edge Bluntness and Slip Flow Effects in High Temperature Hypervelocity Flow over a Flat Plate." General Electric Co. Report No. 62-RL-3006C, Schenectady, New York, 1962.
38. Nagamatsu, H.T., Wisler, D.C. and Sheer, R.E., Jr.
"Circumferential Nonuniform Heating During Transition on a Slender Cone at Hypersonic Mach Numbers." General Electric Co. Report No. 67-C-272, Schenectady, New York, 1967.
39. Nagamatsu, H.T., Wisler, D.C. and Sheer, R.E., Jr.
"Hypersonic Laminar and Turbulent Skin Friction and Heat Transfer on a Slender Cone." General Electric Co. Report No. 69-C-098, Schenectady, New York, 1969.

40. Schaefer, L.R., Leone, S.A. and Nagamatsu, H.T. "An Investigation of the Steady-Flow Establishment Time in a 15 degree Half-Angle Conical Nozzle." Paper 82-0186 presented at the AIAA 20th Aerospace Sciences Meeting, Orlando, FL, January 11-14, 1982.
41. Sheer, R.E., Jr. and Nagamatsu, H.T. "Methods for Distinguishing Type of Hypersonic Boundary Layer in Shock Tunnel." Paper 68-50 presented at the AIAA 6th Aerospace Sciences Meeting, New York, January 22-24, 1968.
42. Vidal, R.J. "Model Instrumentation Techniques for Heat Transfer and Force Measurement in a Hypersonic Shock Tunnel." Cornell Aeronautical Laboratory Report No. AD-917-A-1, Buffalo, New York, 1956.

Unpublished Materials

43. Boulahia, A. "Experimental Investigation of the Airflow Behavior in a Mach 22 Conical Nozzle." Master's Thesis, Rensselaer Polytechnic Institute, Troy, New York, 1986.
44. Bushnell, D.M. "Overview: Technology Issues." Presentation at the AIAA Short Course in Hypersonics. Buffalo, New York, August 19-22, 1986.
45. Hendershot, K.C. "Ground Test Measurements in Hypersonic Facilities." Presentation at the AIAA Short Course in Hypersonics. Buffalo, New York, August 19-22, 1986.
46. Missoum, A. "Experimental Investigation of the Characteristics of the Airflow in a Mach 10 Hypersonic Nozzle." Master's Thesis, Rensselaer Polytechnic Institute, Troy, New York, 1986.
47. Whittliff, C.E. "Short Duration Facilities." Presentation at the AIAA Short Course in Hypersonics. Buffalo, New York, August 19-22, 1986.

END

DATE

FILMED

8-88

DTIC